Fusing Phenomenon of Lithium-Ion Battery Internal Short Circuit

Mingxuan Zhang,[a,b,z] Lishuo Liu,[a] Anna Stefanopoulou,[b,*] Janson Siegel,[b,*] Languang Lu,[a] Xiangming He,[c] and Minggao Ouyang[a,z]

[a]*State Key Laboratory of Automotive Safety and Energy, Tsinghua University, Beijing 100084, People's Republic of China*
[b]*College of Engineering, University of Michigan, Ann Arbor, Michigan 48109, USA*
[c]*Institute of Nuclear and New Energy Technology, Tsinghua University, Beijing 100084, People's Republic of China*

Internal short circuit (ISCr) is one of the major reasons for lithium-ion battery thermal runaway. A new phenomenon, named as the Fusing Phenomenon, is observed during the ISCr experiments. During the Fusing Phenomenon, the ISCr current path will melt down due to the Joule heat of the short current and the ISCr process will be interrupted. The Fusing Phenomenon raises the re-ISCr problem, which means that the battery may have an ISCr again after the end of the former ISCr process. The Fusing Phenomenon's life cycle is given by the hypothesis, which includes the heating-melting period, the ion discharging period and the implosion period. The heating-melting period is analyzed using an axisymmetric local ISCr model. When the ISCr area radius increases, the ISCr current path melting position will change from the ISCr area to the ISCr area edge of the aluminum current collector. If the ISCr area radius is large enough, the battery will run into the thermal runaway instead of the Fusing Phenomenon. The influence factors of the Fusing Phenomenon, including the ISCr area radius and the ISCr material, are analyzed. This research provides new insights on the battery ISCr and enriches our understanding of the ISCr process.

Manuscript submitted July 20, 2017; revised manuscript received August 28, 2017. Published September 9, 2017.

The safety accidents of lithium-ion battery happened one after another, which raises great attention from both society and industry. Internal short circuit (ISCr) is regarded as one of the major safety risks for the lithium-ion batteries. While most of the ISCr incidents only result in poor battery performance, some of them do lead to the thermal runaway and may further results in fatal accidents,[1,2] which are unaffordable for consumers. A thorough understanding of the ISCr is one of the key steps to improving the safety and reliability of the lithium-ion batteries and battery systems.

The self-induced ISCr usually originates from the lithium plating/dendrite, metal impurities and manufacturing defects.[3,4] These elements may establish electron conduction between the positive part and the negative part inside the batteries, which is the case of ISCr. There are 4 types of ISCr, the Cathode-Anode ISCr, the Aluminum-Anode ISCr, the Cathode-Copper ISCr and the Aluminum-Copper ISCr, in which one side belongs to the positive part and the other side belongs to the negative part.[5] Once the ISCr appears, the OCV will decrease due to both the current shunting via ISCr (the Parameter Effect of ISCr) and the self-discharging by ISCr (the Depleting Effect of ISCr).[6] According to the Joule Law, the ISCr current will release the Joule heat. If the heat dissipation capability of the battery is not sufficient, the temperature of the battery will rise up. The continuous increase of temperature will eventually initiate the chain reactions of the thermal runaway.[7]

To repeat the ISCr in the laboratories, several experiment methods were developed by researchers. These methods could be divided into three types according to their action patterns. The first type is the forced pressing method, including the J. Jeevarajan et al.'s round rod crush test,[8] the J. T. Chapin et al.'s blunt nail test,[9–11] the W. Cai et al.'s automated pinch test,[12] the Battery Association of Japan (BAJ) particle-compress test.[13] The BAJ particle-compress test initiates the ISCr by compressing the battery in which a nickel particle is implanted, while the other three methods initiate the ISCr by directly pinching the batteries. The second type is the area-contact method, including the M. Keyser et al.'s phase change material (PCM) trigger method[14,15] and the P. Ramadass et al.'s hole-compress method.[16,17] These methods have a covered hole on battery separator, the M. Keyser et al.'s cover is the PCM, the P. Ramadass et al.'s cover is the insulating film. During the tests, the cover is melted or removed, then the battery positive part and the battery negative part have area-contact through the hole of the separator. The third type is the dendrite growth method, including the C. J. Orendorff et al.'s method[18–20] and the C. McCoy et al.'s method.[21] These methods suggest to implant metallic contaminations or particles into batteries and induce the dendrite growth through the media like sonication, thermal ramp, overcharge, heating and repeated charge/discharge.

ISCr simulation models were developed by researchers basing on the thermal framework, which may include the battery heat generation part, the thermal transfer part, and the measured data. In these models, the ISCr will generate the Joule heat at the beginning period of ISCr. With the temperature increasing, the entropy heat will be released, and the thermal abuse reactions will be ignited once the temperature reaches their thresholds.[22–25] S. Santhanagopalan et al. proposed a typical ISCr model based on the thermal framework and the porous electrode theory.[5] They analyzed the influence factors of ISCr through the model, including the ISCr type, the electrode lithiation, the ISCr area, the initial temperature, the battery capacity, the SOC and the oxygen availability. W. Fang et al. reported an ISCr model using the measured data as boundary conditions.[17] H. Maleki et al. developed an ISCr model based on the measured profiles of electrical, electrochemical and chemical heat generation.[1] T. G. Zavalis et al. constructed an axisymmetric one layer model for the Cathode-Anode type ISCr and analyzed the behavior of the external short circuit, nail penetration and impurity-induced ISCr.[26]

Those experiments and simulations enlighten our insight on the battery ISCr. However, most of the existing ISCr experiment methods are implemented with forced method or area contact and the existing ISCr simulation models take the ISCr as a continuous process, both of them lead to the missing of details related to the fact that some of the ISCr has point contact at the ISCr spot rather than area contact and there is the possibility of discontinuity of ISCr in practice.

In our previous work, a novel ISCr experiment method, the shape memory alloy (SMA) ISCr trigger method is introduced.[27] The SMA ISCr trigger has very small dimensions (0.2 mm thickness and less than 0.5 cm^2 area) and can be easily implanted into the battery cell. It has a sharp arrow which will function to penetrate separator when it reaches the critical temperature of the SMA. The SMA ISCr trigger method has little influence on the battery performance and can initiate the ISCr of different types. Different to the existing ISCr experiment methods, the SMA ISCr trigger method creates point contact in short area without externally forced measures.

*Electrochemical Society Member.
[z]E-mail: ouymg@tsinghua.edu.cn; zhangmx13@mails.tsinghua.edu.cn

Table I. Information of the Experiment Batteries.

Parameter	Value	Unit
Cathode	NCM	-
Type	Prismatic Pouch	-
L × W × H	60 × 50 × 4	mm
Cell	Jelly-Roll (Wound)	-
Capacity	1	Ah
Thickness of Cathode, d_{Ca}	92	μm
Thickness of Anode, d_{An}	98	μm
Thickness of Separator, d_{Sp}	17	μm
Thickness of Aluminum, d_{Al}	15	μm
Thickness of Copper, d_{Cu}	10	μm
Internal Resistance, R_{inner}	32.5	mΩ

In this research, a new phenomenon, named as the Fusing Phenomenon of ISCr, is observed during the Aluminum-Copper ISCr. The Fusing Phenomenon of ISCr refers to the interruption of the ISCr process due to the fusing (melting) of the ISCr current path. It could be the similar case implied by the Panasonic's ISCr detection patents, in which the drop and recovery feature of the battery terminal voltage are taken as the criterion of the ISCr detection.[28] Panasonic suggested that the battery terminal voltage will drop suddenly due to the ISCr, then the large ISCr current will burn down the Aluminum and further lead to the interruption of ISCr as well as the recovery of the battery terminal voltage.

In this work, the SMA ISCr trigger method is employed to observe the Fusing Phenomenon of ISCr during the Aluminum-Copper ISCr. An axisymmetric local model is established to explain and analyze the Fusing Phenomenon at the ISCr spot. In Experimental evidence of fusing phenomenon section, the experiments on the Aluminum-Copper ISCr are conducted using the area contact method and the point contact method separately. The Fusing Phenomenon is observed during the experiment using the point contact method. A case in which the re-ISCr occurred after the interruption of ISCr is provided and the Fusing Phenomenon's life cycle is given by the hypothesis. In Computational analyses of the fusing phenomenon of ISCr section, the axisymmetric local ISCr model is established and used to analyze the Fusing Phenomenon. In Influence factors of the fusing phenomenon section, the influence factors of the Fusing Phenomenon are analyzed using the axisymmetric local ISCr model. Finally, the summaries and conclusions are presented in Discussion and conclusions section.

Experimental Evidence of Fusing Phenomenon

In this research, the 1Ah NCM lithium-ion pouch batteries fabricated by Jiangsu Huadong Institute of Li-ion Battery (JHILB) are used as the research object. All of the experimental batteries were fabricated by cooperating with JHILB. The information of this type battery is listed in Table I.

The aluminum-copper ISCr using the NREL PCM method.— The NREL PCM ISCr trigger method initiates the battery ISCr by creating area contact between the battery negative part and the battery positive part at the ISCr area, and yields continuous ISCr process. This method is employed to trigger the Aluminum-Copper ISCr for comparing with the SMA ISCr trigger method, which creates point contact at the ISCr area. Two experimental batteries, Al-Cu_PCM1 and Al-Cu_PCM2, are fabricated and heated to the phase change temperature of the PCM (non-crystalline, melt around 40∼50°C) to initiate ISCr. The terminal voltages and temperature profiles of the experimental batteries are shown in Figure 1. The terminal voltages drop to 1 V once the ISCr begins and then quickly decline to 0 V, meanwhile the temperatures rise up to 107°C instantly. The laminated pouches are inflated up, but no explosion, smoking or leakage happens.

The aluminum-copper ISCr using the SMA ISCr trigger method.—The SMA ISCr trigger can change its shape due to the shape memory effect[29] and will penetrate battery separator when it reaches its function temperature (70°C). It has small dimension and

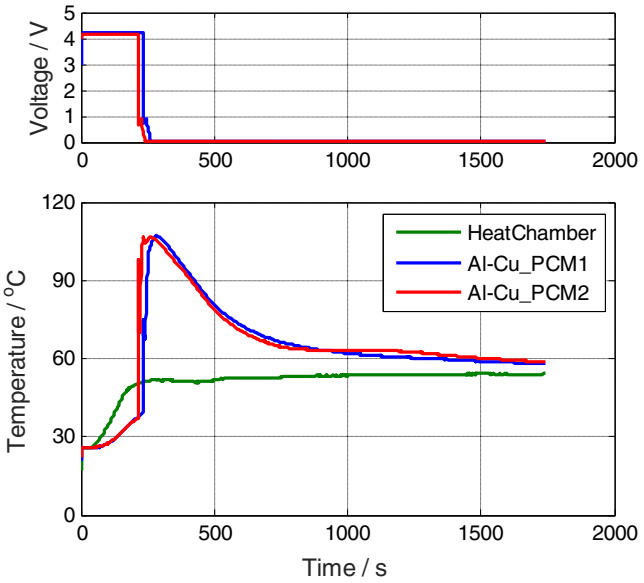

Figure 1. The terminal voltage and temperature profiles of the Aluminum-Copper ISCr experiments using the NREL PCM method.

can be implanted into batteries to trigger different types of ISCr on demand while keeping the integrity of the battery.

At first, the experimental batteries with the SMA ISCr triggers are fabricated for the Aluminum-Copper ISCr experiments. The experimental batteries output stable terminal voltage without decline after initiating the Aluminum-Copper ISCr. The disassembling results show that the SMA ISCr triggers have already penetrated the separator and confirmed that the ISCr have been initiated. With this results, it is suggested that the large ISCr current burns down the ISCr current path instantaneously by the Joule heat, thus the terminal voltage could remain stable after the SMA ISCr triggers penetrated the separator. This scenario is similar to the fusing process, in which the fuse material is melted down by the huge current. In the Aluminum-Copper ISCr case, the Aluminum current collector and the Copper current collector are connected together via the lithium dendrite and other impurities in practice or the arrow of the SMA ISCr trigger in experiments. Given the huge short circuit current, the ISCr current path of the Aluminum-Copper ISCr could be burnt down quickly by the Joule heat.

One common appearance of the current path burning down is the electric sparks. If the ISCr current path does be burnt down by the huge short circuit current, the electric spark can be observed during the Aluminum-Copper ISCr. To verify the conjecture, a special experimental battery for the Aluminum-Copper ISCr is fabricated, in which an SMA ISCr trigger is implanted in the outermost cycle of the jelly-roll and is strong enough to penetrate the aluminum laminated film pouch of the battery to expose the ISCr spot when initiating the ISCr. Once the experimental battery is heated up to the functioning temperature of the SMA ISCr trigger, the trigger's arrow will initiate the Aluminum-Copper ISCr and penetrate the laminated shell at the same time. Therefore, if there are sparks from current path burning down at the ISCr spot, they will be exposed and can be observed.

The special experimental battery is heated up using the hot wind gun in open space in order to capture visual results. Figure 2 shows the terminal voltage profile and the photo of electric spark at the ISCr spot during the Aluminum-Copper ISCr. The aluminum laminated film pouch itself is electrically insulated from the battery jelly-roll, and one-spot connect with the penetrated position will result in neither the short circuit current nor the electric spark. The only possible origin of the electric spark is the ISCr current from the Aluminum-Copper ISCr. Besides, the flat terminal voltage curve (1 Hz sampling frequency) indicates there is no continuous short circuit inside the

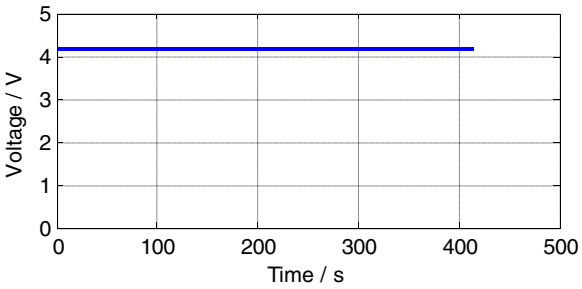

(a)

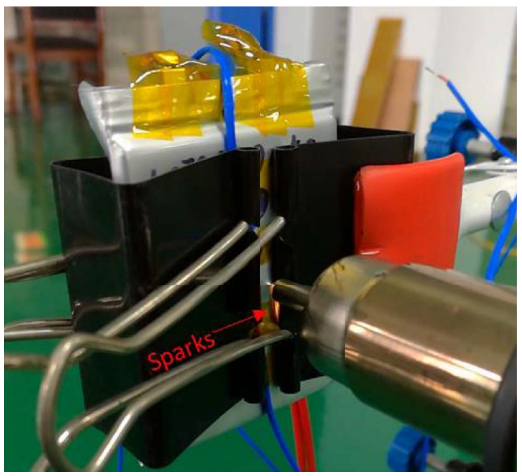

(b)

Figure 2. The Aluminum-Copper ISCr experiment using the SMA ISCr trigger method, heated by hot wind gun. (a) – The terminal voltage profile, no voltage drop is captured; (b) – Sparks during the Aluminum-Copper ISCr.

battery, if not, the terminal voltage will drop dramatically due to the ISCr. This result matches with the conjecture that the ISCr current path of the Aluminum-Copper ISCr is burnt down by the huge short circuit current. This phenomenon is named as Fusing Phenomenon of ISCr, regarding of the similarities between it and the fusing process. The lasting time of the Fusing Phenomenon is pretty short and less than the sampling period, otherwise, the voltage change during the ISCr period would be recorded by the signal recorder. The sampling frequency of the terminal voltage is 1 Hz, then the lasting time of the Fusing Phenomenon should be less than 1 s.

The re-ISCr after the fusing phenomenon.—The ISCr process may be interrupted by the Fusing Phenomenon of ISCr. But the breaches in battery structure created by the ISCr and the Fusing Phenomenon will remain, which would give a chance to the re-ISCr. Whether the battery will have a re-ISCr after the Fusing Phenomenon does make great differences in the battery safety strategies. If there is no chance of the re-ISCr, then the batteries could be allowed to work after the Fusing Phenomenon. However, if there is a possibility of re-ISCr, the batteries who have got the Fusing Phenomenon must be removed from the battery system as soon as possible and the detection of the Fusing Phenomenon will be necessary for the battery safety strategies.

By chance, a re-ISCr case is recorded in this research. The object is an experimental battery with the SMA ISCr trigger for the Aluminum-Copper ISCr. It is heated up to the functioning temperature of the SMA ISCr trigger (70°C). The Aluminum-Copper ISCr should have been initiated once the battery temperature reaches the functioning temperature. Figure 3 shows the terminal voltage and temperature profiles. Just like the other Aluminum-Copper ISCr experiments conducted by the SMA ISCr trigger method, this battery doesn't yield continuous ISCr at the functioning temperature. But after cooling down and a

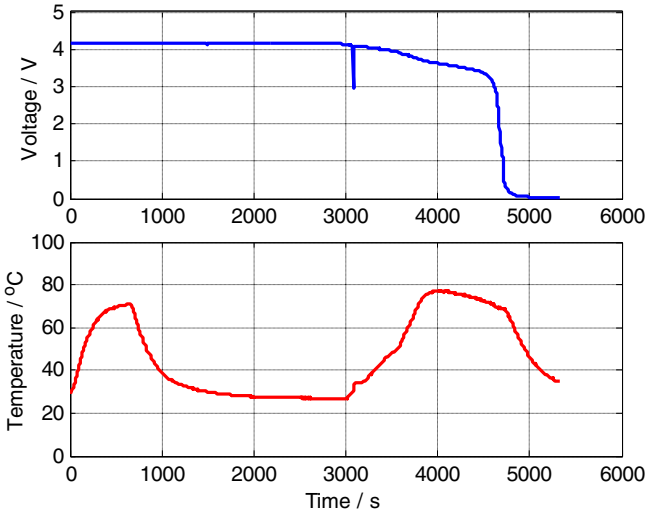

Figure 3. The terminal voltage and temperature profiles of the Aluminum-Copper ISCr experiments using the SMA ISCr trigger method. A re-ISCr case is captured.

period of waiting, it happens to get the re-ISCr spontaneously. At the time 2996 s, the terminal voltage begins to decrease slowly and the battery temperature begins to increase. And 83 s later, the battery has a sharp voltage drop-recovery. This sharp voltage drop-recovery is only recorded by one sampling point and can possibly indicate the Fusing Phenomenon of ISCr. Meanwhile, a corresponding temperature rising peak is captured in the temperature profile. In this case, the sharp voltage drop-recovery interrupts the severe process of the ISCr with low resistance (could be the Aluminum-Copper ISCr) but doesn't shut down the slow re-ISCr process which may be the ISCr of other types. Finally, the battery is totally discharged by the re-ISCr and has the maximum temperature of 77.5°C.

Hypothesis for the fusing phenomenon.—The entire Fusing Phenomenon life cycle is divided into three periods, the heating-melting period, the ion discharging period and the implosion period.

In the heating-melting period, the ISCr current path inside the battery is heated up by the Joule heat of the huge short circuit current. Once a certain position of the ISCr current path reaches its material's melting point, it will melt down and further cut off the ISCr current path.

In the ion discharging period, the running electron flow is cut off by the melting down of the ISCr current path and micro gaps will emerge in the cutoff position once the material melts down. The ISCr current could be up to hundreds C-rate and the instant cutting off will result in the voltage surge. The potential of the voltage surge will be much larger than the original circuit potential and imposed on the cutoff position of the ISCr current path. With the small dimension of the gap in the cutoff position, magnificent potential gradient could be expected, which will ionize the insulating media in the gaps and lead to ion discharging.

In the implosion period, with the ion discharging and time passing, the voltage surge will fade away and the ion discharging will stop. The temperature of the ion discharging channel could be very high during the ion discharging period. Once the ion discharging stops, the implosion will happen due to the dramatical temperature drop. The implosion will worsen the adjacent battery structure and increase the potential of the re-ISCr, like the case presented in The re-ISCr after the fusing phenomenon section.

The heating-melting period of the Fusing Phenomenon is proven and analyzed in the following sections through the computational model. However, the ion discharging period and the implosion period are beyond the present measurement and calculation capability in our laboratory, thus presented in hypothesis form.

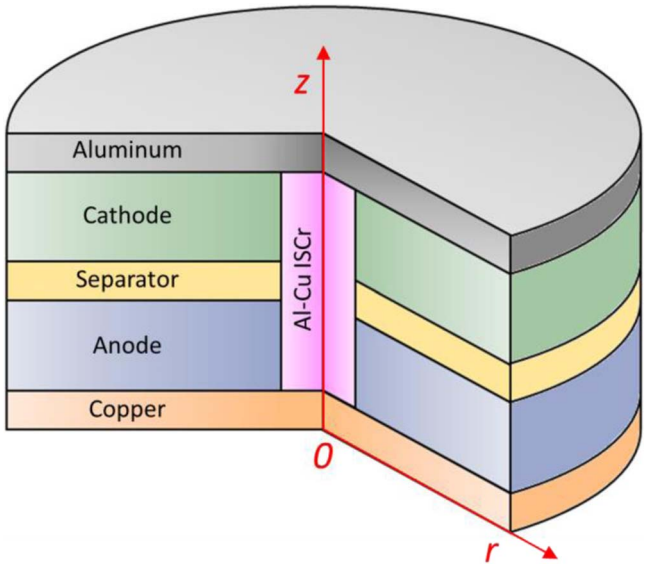

Figure 4. Sketch of the axisymmetric local ISCr model of the Aluminum-Copper ISCr.

Computational Analyses of the Fusing Phenomenon of ISCr

The following analyses have the time scales of fractions of a millisecond to several milliseconds. The corresponding assumptions are made upon the fact of the short time duration.

Axisymmetric local ISCr model of the aluminum-copper ISCr.— To analyze the Fusing Phenomenon of ISCr, an axisymmetric local ISCr model for the Aluminum-Copper ISCr is established. Normally, there are three heat calculation parts for the battery heat simulation models, which are the thermal abuse reaction heat part, the entropy heat part, and the Joule heat part. However, for the Fusing Phenomenon, it is known from the experiment results that there is no thermal runaway, no obvious self-heating, and everything happens within a short time duration. Meanwhile, the thermal abuse reaction heat part and the entropy heat part require high temperature or temperature increase to function. Therefore, the thermal abuse reaction part and the entropy heat part are not included in the axisymmetric local ISCr model, and the heat generation is calculated through the Joule Law.

Joint Research Center of European Commission studied the external short circuit (ESCr) behavior of NCM batteries and they suggested that the batteries' double layer capacitance is dominant in the initial period of ESCr and the short current is limited by the external resistance, given by Equation 3.[30] Both the ISCr and the ESCr share the similar discharging principle in their initial period and the Fusing Phenomenon happens in the initial period of the ISCr. Therefore, in this research, the short current of the Fusing Phenomenon is treated as following the same principle with the ESCr and is calculated by Equation 3. It is assumed that the battery elements are adiabatic and the ion concentration is constant due to the short time duration. Table I provides the battery's geometric information, and the model's geometrical sketch is shown in Figure 4. The model's governing equations and parameters are presented in Table II and Table III.[31,32]

Table II. Governing Equations of the Axisymmetric Local ISCr Model.

Equations		
Joule heat	$q_j = \frac{(j_s)^2}{\sigma^{eff}} + \frac{(j_e)^2}{\kappa^{eff}}$	[1]
Temperature	$\frac{\partial(\rho C_p T)}{\partial t} = q_j$	[2]
Short circuit current	$I_{ISCr} = I_{max}\frac{1}{1+R_{ISCr}/R_{inner}}$	[3]
Effective solid electrical conductivity	$\sigma^{eff} = \sigma(1-\varepsilon_e)$	[4]
Effective electrolyte ionic conductivity	$\kappa^{eff} = \kappa\varepsilon_e$	[5]
ISCr resistance	$R_{ISCr} = \frac{h}{\pi {r_{ISCr}}^2 \sigma_{ISCr}}$	[6]

Table III. Parameters of the Axisymmetric Local ISCr Model.

Parameter	Cathode	Separator	Anode
Solid electrical conductivity, σ, S m^{-1}	10	-	100
Density, ρ, kg m^{-3}	2860	525	1200
Specific heat, C_p, J kg^{-1} K^{-1}	1150	2050	1150
Porosity, ε_e	0.27	0.32	0t2.27
Electrolyte ionic conductivity, κ, S m^{-1}	$0.041253 + 0.5007\frac{c}{1000} - 0.47212(\frac{c}{1000})^2 + 0.15094(\frac{c}{1000})^3 - 0.016018(\frac{c}{1000})^4$[31]		
Electrolyte concentration, c, mol m^{-3}	1200		
Maximum current, I_{max}	250 C-rate[30]		
Initial temperature, T_0,°C	25		

All the parameters without references are adopted from Ref. 32 or estimated.

The axisymmetric local ISCr model ends under two conditions. The first condition: once the current collectors or the ISCr reach their melting point, the ISCr current path will be cut off. The second condition: once the electrodes reach the ignition temperature of the battery thermal abuse reactions, the self-driven thermal abuse reactions will start and the battery may run into thermal runaway. The melting points of the current collectors, the melting point of the ISCr and the ignition temperature of the battery thermal abuse reactions are the critical temperatures, beyond which the ISCr process will whether be cut off or turn into the thermal runaway. The physical parameters of the potential ISCr materials are listed in Table IV. The thermal abuse reaction with the lowest ignition temperature is the SEI decomposition reaction, which has the ignition temperature around 100°C.[33] The temperature is calculated using the axisymmetric local ISCr model of the Aluminum-Copper ISCr until one of the critical temperatures is reached.[34]

Simulation analysis of the fusing phenomenon.— The Aluminum-Copper ISCr of aluminum, in which the ISCr material is aluminum, is simulated using the axisymmetric local ISCr model. Figure 5a presents the schematic of the currents distribution in the ISCr area and its vicinity. The currents flow through the electrodes

Table IV. Physical Parameters of the ISCr Materials.

Parameter	Aluminum	Copper	Lithium	Iron	Magnesium
Electrical conductivity, σ, S m^{-1}	37.7×10^6	59.6×10^6	10.8×10^6	9.93×10^6	22.6×10^6
Density, ρ, kg m^{-3}	2712	8940	534	7850	1738
Specific heat, C_p, J kg^{-1} K^{-1}	897	385	3582	449	1050
Melting point, T_m,°C	660	1083	181	1535	649

All the parameters are adopted from Ref. 34.

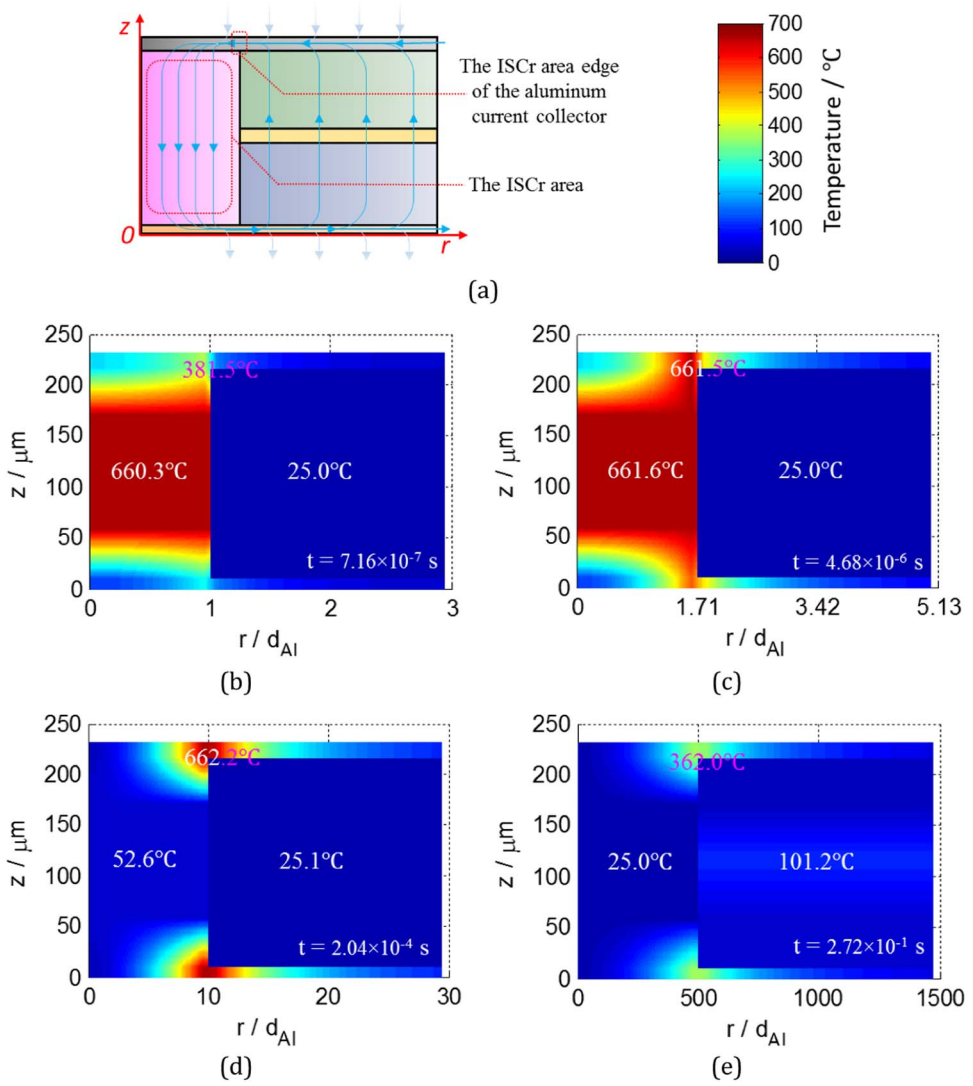

Figure 5. Simulation results of the axisymmetric local ISCr model of the Aluminum-Copper ISCr of aluminum. (a) The schematic of the current distribution in the ISCr area and its vicinity; Temperature distribution map of the ISCr area and its vicinity when (b) $r_{ISCr} = 1\ d_{Al}$; (c) $r_{ISCr} = 1.71\ d_{Al}$; (d) $r_{ISCr} = 10\ d_{Al}$; (e) $r_{ISCr} = 500\ d_{Al}$.

and separator, then gather on the current collectors and further flow through the ISCr area. The ISCr area always has the entire ISCr currents flowing through. Therefore, if the ISCr area radius is small enough, the current density will be very high and the huge Joule heat will melt down the ISCr area quickly. Besides, all of the ISCr currents also have to cross the ISCr area edge of the current collectors, which results in that the ISCr area edge of the current collectors has the maximum current density in the current collectors. Therefore, the ISCr area edge of the aluminum current collector (EdgeAl) is the most vulnerable position in the current collectors, given that the melting point of aluminum is much lower than copper's.

Figures 5b∼5e shows the temperature distribution under different ISCr area radius. The radius coordinate is measured by the unit, d_{Al}, which is the thickness of the aluminum current collector. The maximum temperatures in the ISCr area, the ISCr area EdgeAl and the electrodes are marked on the figures. The critical times, which indicates the time for the battery to reach one of its critical temperatures, are also marked in the figures.

Figure 5b shows the case of $r_{ISCr} = 1\ d_{Al}$. After 7.16×10^{-7} s, the ISCr area reaches its critical temperature of 660°C. Then the ISCr area will melt down and the ISCr current path will be cut off. Figure 5c shows the case of $r_{ISCr} = 1.71\ d_{Al}$. After 4.68×10^{-6} s, the ISCr area and the ISCr area EdgeAl reach their critical temperature of 660°C at the same time. Then the ISCr area and the ISCr area EdgeAl will melt down and the ISCr current path will be cut off. Figure 5d shows the case of $r_{ISCr} = 10\ d_{Al}$. After 7.16×10^{-7} s, the ISCr area EdgeAl reaches its critical temperature of 660°C. Then the ISCr area EdgeAl will melt down and the ISCr current path will be cut off.

In these three case, the ISCr area or the ISCr area EdgeAl reach their critical temperatures in very short time durations (the longest one is 0.204 ms). The electrodes do not have sufficient time to be heated up before the ISCr current path is cut off and the thermal abuse reactions will not be ignited.

Compared with the ISCr area, the electrode has significantly larger size and thus has smaller current density. However, the relatively poor conductivity of the electrode will amplify the current's Joule effect and the electrode may have a chance to reach its critical temperature before the ISCr current path melting down. If the radius of the ISCr area increases, the current densities in both the ISCr area and the ISCr area EdgeAl will decrease and it will require a longer time to reach their critical temperatures. Once the radius of the ISCr area is large enough, the electrode will be heated up to its critical temperature before the ISCr current path melting down. Figure 5d shows the case of $r_{ISCr} = 500\ d_{Al}$, the electrode reaches its critical temperature of

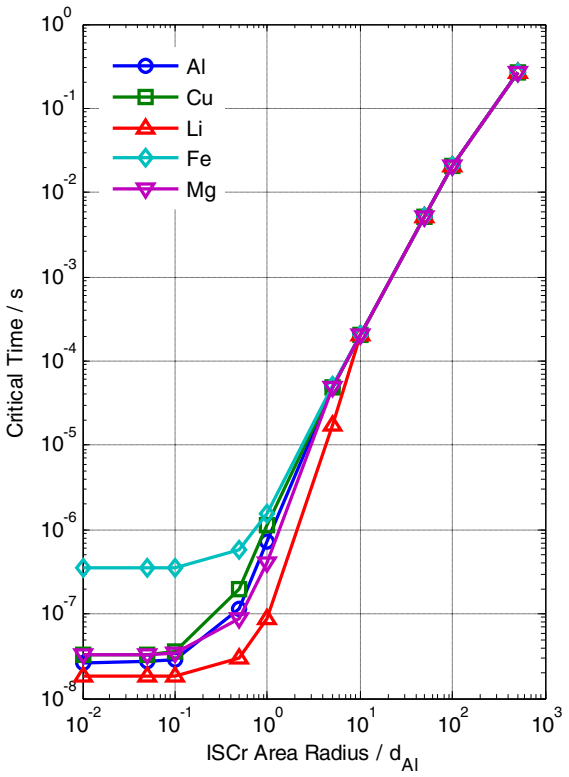

Figure 6. The critical time vs. ISCr area radius curve in the logarithmic coordinate. "d_{Al}" is the thickness of the aluminum current collector which is 1.5×10^{-2} mm.

100°C after 0.272 s while the ISCr area and the ISCr area EdgeAl are still under their critical temperatures. It should be stressed that the time duration in this case is too long to support the adiabatic assumption and the short circuit current's calculation principle. Therefore, the results from the case of $r_{ISCr} = 500\ d_{Al}$ cannot be used for quantitative analyses.

Influence Factors of the Fusing Phenomenon

ISCr area radius.—As shown in Simulation analysis of the fusing phenomenon section, the ISCr area radius will substantially influence the Aluminum-Copper ISCr process. The pores in the battery porous separator provide the available spaces and paths to the growth of the metal dendrites, which is regarded as one of the origins of the battery ISCr. The diameter of the pores is around $10^{-8} \sim 10^{-7}$ m magnitude[35] and could be regarded as the basic ISCr area radius. The ISCr area radius may increase due to the metal impurities, the defect of the separator, the growth of the metal dendrites, etc. Once the ISCr area radius is large enough, neither the ISCr area nor the ISCr area EdgeAl will melt before the electrode reaches its critical temperature, then happens the battery thermal runaway instead of the Fusing Phenomenon. Therefore, the influence of the ISCr area radius is studied from the 10^{-7} m magnitude (0.01 d_{Al}) to the 10^{-3} m magnitude (500 d_{Al}).

Figure 6 shows the critical time vs. ISCr area radius curves in the logarithmic coordinate and Table V presents the ISCr current path melting types under each ISCr area radius. Along the increase of the ISCr area radius, the critical time increases and the ISCr current path melting type changes from IM (the ISCr area melts down) to AM (the ISCr area EdgeAl melts down) and finally to AR (the thermal abuse reactions start). The r_1 denotes the ISCr area radius under which the ISCr area and the ISCr area EdgeAl will melt at the same time. The r_2 denotes the ISCr area radius under which the melting of the ISCr area EdgeAl and the thermal abuse reactions of electrodes will happen at the same time.

Figure 7 shows the average current density of the Aluminum-Copper ISCr of aluminum. Under the small ISCr area radius (R_{ISCr} is large), the short circuit current is restricted by the material conductivities and the current density in ISCr area doesn't change much when the ISCr area radius changes. Besides, the current density in the ISCr area EdgeAl is much smaller than in the ISCr area. Therefore, the critical time with little changing and the result of IM could be expected for the small ISCr area radius. Along the increasing of the ISCr area radius, the total short circuit current increases and the battery double layers capacitance starts to restrict the total short circuit current. Then the current density in the ISCr area begins to decrease along the increasing of the ISCr area radius. The current density in the ISCr area EdgeAl increases at first because its area increasing speed is slower than the ISCr area, but finally, it begins to decrease due to the restriction on the total short circuit current from the battery double layers capacitance. The current density in the ISCr area EdgeAl will surpass the current density in the ISCr area along the ISCr area radius increasing. Correspondingly, the ISCr with larger ISCr area radius will have longer critical time and the result of AM. If the ISCr area radius is large enough, the current density in both the ISCr area and the ISCr area EdgeAl will be too low to heat up their own position in short time. With the time increase, the electrode will be heated up to its critical temperature and the thermal abuse reactions will be ignited. As stressed in Simulation analysis of the fusing phenomenon section, the results for the r_2 case and the $r_{ISCr} = 500\ d_{Al}$ case cannot be used as quantitative analyses because its long time duration doesn't meet the prerequisites of the axisymmetric local ISCr model.

Table V. Short circuit current Path Melting Types.

ISCr Area Radius / mm	Aluminum	Copper	Lithium	Iron	Magnesium
0.01 d_{Al}= 1.5×10^{-4}	IM	AM	IM	IM	IM
0.05 d_{Al}= 7.5×10^{-4}	IM	AM	IM	IM	IM
0.1 d_{Al}= 1.5×10^{-3}	IM	AM	IM	IM	IM
0.5 d_{Al}= 7.5×10^{-3}	IM	AM	IM	IM	IM
1 d_{Al}= 1.5×10^{-2}	IM	AM	IM	IM	IM
5 d_{Al}= 7.5×10^{-2}	AM	AM	IM	AM	AM
10 d_{Al}= 1.5×10^{-1}	AM	AM	AM	AM	AM
50 d_{Al}= 7.5×10^{-1}	AM	AM	AM	AM	AM
100 d_{Al}= 1.5	AM	AM	AM	AM	AM
500 d_{Al}= 7.5	AR	AR	AR	AR	AR
r_1 / mm	$1.71d_{Al} = 2.57 \times 10^{-2}$	-	$8.83d_{Al} = 0.132$	$1.84d_{Al} = 2.76 \times 10^{-2}$	$2.91d_{Al} = 4.37 \times 10^{-2}$
r_2 / mm	$364d_{Al} = 5.46$	$364d_{Al} = 5.46$	$364d_{Al} = 5.46$	$364d_{Al} = 5.46$	$364d_{Al} = 5.46$

Note: IM – the ISCr area melts down; AM – the ISCr area EdgeAl melts down; AR – the thermal abuse reactions start. r_1 is the radius in which the ISCr area and the ISCr area EdgeAl melt at the same time. r_1 is the radius in which the ISCr area EdgeAl melts and the thermal abuse reactions start at the same time.

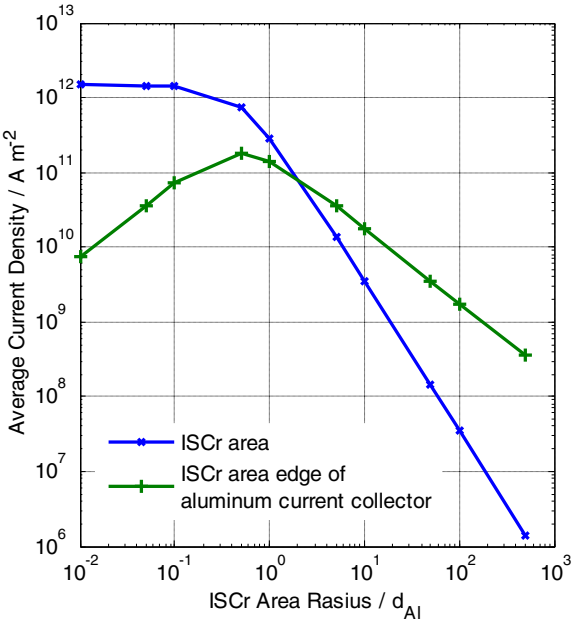

Figure 7. The average current density in the ISCr area and the ISCr area EdgeAl during the Aluminum-Copper ISCr of aluminum

ISCr material.—Aluminum and copper are the material of the lithium battery current collectors and thus are possible impurities inside batteries. Lithium is one of the major elements in lithium batteries and can form dendrite inside batteries. Iron and magnesium are potential impurities from the factory production lines and manufacturing equipment. Therefore, aluminum, copper, lithium, iron, and magnesium are taken as the ISCr materials of the Aluminum-Copper ISCr.

The conductivity, the heat capacity and the melting point of the ISCr material may influence the Aluminum-Copper ISCr process. The higher the conductivity is, the higher the total short circuit current is, but less Joule heat under the same current density. The higher the heat capacity is, the less temperature rising under the same quantity of heat. The higher the melting point is, the larger temperature increase is required to melt down the ISCr area.

Once the ISCr area radius is above 10 d_{Al}, all of the Aluminum-Copper ISCr of the five ISCr materials have almost the same critical time and short circuit current path melting types, as shown in Figure 6 and Table V. The reason is that the ISCr area radius is already large enough to have a very small R_{ISCr}, and the total short circuit current depends on the I_{max}. Then the ISCr process is majorly determined by the feature of the battery itself instead of the ISCr materials. As for the cases whose ISCr area radius is smaller than 10 d_{Al}, the influence of the ISCr materials will emerge.

Magnesium and aluminum are very similar in many aspects. Therefore, the Aluminum-Copper ISCr of magnesium also has similar features with the Aluminum-Copper ISCr of aluminum.

Copper has similar "critical time – ISCr area radius" curve with aluminum and magnesium, as shown in Figure 6. But the ISCr current path melting types of copper are quite different from aluminum and magnesium, as shown in Table V. For copper, in the range of 0.01 d_{Al} to 100 d_{Al}, the melting type is always AM. Given that the melting point of copper is higher than aluminum, the ISCr area EdgeAl will melt down first instead of the ISCr area of copper. Because the Aluminum-Copper ISCr of copper always has the result of AM, it doesn't have an r_1.

Lithium has a melting point of 181°C, which is the lowest among the five ISCr materials. The low melting point makes it very easy to melt down the lithium ISCr area during the ISCr process. Therefore, the short critical times and the large r_1 could be expected for the Aluminum-Copper ISCr of lithium, as shown in Figure 6 and Table V.

Iron has the highest melting point among the five ISCr materials, but it doesn't lead to pure AM type of melting like copper. In fact, iron has the similar melting types with aluminum and magnesium. Different from copper, iron has a conductivity lower than aluminum. This results in that the ISCr area of iron is heated up faster than the ISCr area EdgeAl under the same current density. But given that the high melting point of iron, the Aluminum-Copper ISCr of iron has longer critical time than the Aluminum-Copper ISCr of other ISCr materials.

Discussion and Conclusions

The Aluminum-Copper ISCr experiments are conducted using the NREL PCM method and the SMA ISCr trigger method. The experiments using the NREL PCM method create surface contact at the ISCr area and yield the continuous ISCr results. While the experiments using the SMA ISCr trigger method create point contact at the ISCr area and do not yield the continuous ISCr results. The dissembling results of the experimental batteries using the SMA ISCr trigger method show that the SMA ISCr triggers have been already initiated and there are burning traces in the ISCr area. It is suggested that the ISCr current path might be instantly burnt down by the Joule heat of the huge short circuit current, which is similar to the fusing process and is named as the Fusing Phenomenon of ISCr. To verify the Fusing Phenomenon of ISCr, a special battery is fabricated, in which the SMA ISCr trigger is placed at the outermost layer and can penetrate the battery laminated shell while initiating the Aluminum-Copper ISCr. The electrical sparks are captured when the Aluminum-Copper ISCr is initiated and indicate the burning down of the ISCr current path, meanwhile, the measured terminal voltage remains unchanged. The results are consistent with the Fusing Phenomenon of ISCr.

The Fusing Phenomenon of ISCr may interrupt the ISCr process but leaves or even increases the chances of re-ISCr by worsening the battery structure in the original ISCr area. A re-ISCr case is recorded in this research. After initiation of the Aluminum-Copper ISCr, the experimental battery's terminal voltage remains stable. However, after about half an hour waiting, the battery gets the re-ISCr spontaneously, its terminal voltage begins to decrease and its temperature starts to increase slowly. A voltage drop-recovery case, which may originate from the Fusing Phenomenon, is captured during the slow re-ISCr process.

The Fusing Phenomenon of ISCr is analyzed through the computational method. The axisymmetric local ISCr model of the Aluminum-Copper ISCr is built to calculate the temperature increase in the ISCr area and its vicinity. For the small ISCr area radius, the ISCr area will melt down first and cut off the ISCr current path. For the relatively large ISCr area radius, the ISCr area EdgeAl will melt down first and cut off the ISCr current path. Once the ISCr current path is cut off, the Aluminum-Copper ISCr process will stop, behaving as the Fusing Phenomenon. If the ISCr area radius is large enough, the thermal abuse reactions will start before the ISCr current path melting down, behaving as the battery thermal runaway.

The life cycle of the Fusing Phenomenon of ISCr is proposed as the hypothesis, which includes the heating-melting period, the ion discharging period and the implosion period. After the ISCr current path melting down, small gaps will emerge at the melting down position and have huge potential gradient due to the voltage surge and the small dimension. The huge potential gradient will ionize the media inside the gaps and lead to the ion discharging. After the voltage surge fading off, the ion discharging will stop, which leads to the implosion due to the dramatical decrease of the temperature in the ion channel. The implosion will worsen the battery structure in the ISCr area, which leaves or even increases the chances of the re-ISCr.

The influence of the ISCr area radius is analyzed using the axisymmetric local ISCr model. The computational results indicate that along the increasing of the ISCr area radius, the melting position would change from the ISCr area to the ISCr area EdgeAl, and the critical time will increase. If the ISCr area radius is large enough, the battery will go into thermal runaway instead of the Fusing Phenomenon.

The influence of the ISCr material is analyzed using the axisymmetric local ISCr model. The Aluminum-Copper ISCr of magnesium has similar behavior with the one of aluminum. For the Aluminum-Copper ISCr of lithium, it is easy to have the ISCr area melting down because of the low melting point of lithium. For the Aluminum-Copper ISCr of copper, the melting position is always the ISCr area EdgeAl no matter how the ISCr area radius changes due to the high melting point of copper. The Aluminum-Copper ISCr of iron has similar melting positions with the one of aluminum when the ISCr area radius changes, but it has longer critical times because of the high melting point of iron.

In conclusion, the Fusing Phenomenon of ISCr is observed during the Aluminum-Copper ISCr using the SMA ISCr trigger method. The Fusing Phenomenon will interrupt the ISCr process but will also leave chances of the re-ISCr. A re-ISCr case is recorded in this research. The heating-melting period of the Fusing Phenomenon is analyzed through the axisymmetric local ISCr model of the Aluminum-Copper ISCr. The computational results show that the ISCr area will melt down in the small ISCr area radius cases while the ISCr area EdgeAl will melt down in the large ISCr area radius cases. If the ISCr area radius is large enough, the battery will go into thermal runaway instead of the Fusing Phenomenon. The life cycle of the Fusing Phenomenon is proposed, which includes the heating-melting period, the ion discharging period and the implosion period. The influences of the ISCr area radius and the ISCr material are analyzed. This research provides new insights on the battery ISCr and enriches our understanding of the ISCr process. The information revealed by the Fusing Phenomenon of ISCr will raise new tasks for the battery safety researchers and the re-ISCr indicates the necessity of the detection of the Fusing Phenomenon.

Acknowledgment

This work is supported by the National Natural Science Foundation of China under the grant No. U1564205 and funded by the Ministry of Science and Technology of China under the grant No. 2016YFE0102200. The first author is funded by China Scholarship Council. The author thank the participating in the experiments of Guohua Li, Chunyan Guo, Jianxun Ren, and Qing Liu from Jiangsu Huadong Institute of Li-ion Battery.

References

1. H. Maleki and J. N. Howard, "Internal Short Circuit in Li-ion Cells," *J. Power Sources*, **191**, 568 (2009).
2. Tesla Model S Battery Cells Explode after Fatal Indianapolis Crash, http://autoweek.com/article/car-news/tesla-model-s-battery-explodes-after-fatal-crash-downtown-indianapolis, Nov. 4, 2016.
3. J. Cannarella and C. B. Arnold, "The Effects of Defects on Localized Plating in Lithium-Ion Batteries," *J. Electrochemical Society*, **162**, 1365 (2015).
4. S. Hwang, *An Overview of Internal Short Circuit Screening Test Methods for Lithium Batteries and a Proposal for Test T.6 Modification, Presentation at 1st Workshop on Lithium Batteries*, Brussels, Belgium, March 17–18, 2015.
5. S. Santhanagopalan, P. Ramadass, and J. Zhang, "Analysis of Internal Short-Circuit in a Lithium ion Cell," *J. Power Sources*, **194**, 550 (2009).
6. M. Ouyang, M. Zhang, X. Feng, L. Lu, J. Li, X. He, and Y. Zheng, "Internal short circuit detection for battery pack using equivalent parameter and consistency method," *J. Power Sources*, **294**, 272 (2015).
7. Q. Wang, P. Ping, X. Zhao, G. Chu, J. Sun, and C. Chen, "Thermal Runaway Caused Fire and Explosion of Lithium Ion Battery," *J. Power Sources*, **208**, 210 (2012).
8. J. Jeevarajan, *Determination of Tolerance to Internal Shorts and Its Screening in Li-Ion Cells - NASA JSC Method, NASA Aerospace Battery Workshop*, Huntsville, AL, 2008.
9. J. T. Chapin and A. Wu, *Blunt Nail Crush Internal Short Circuit Lithium-ion Cell Test Method*, NASA Aerospace Battery Workshop, Huntsville, AL, 2009.
10. H. P. Jones, J. T. Chapin, and M. Tabaddor, Critical Review of Commercial Secondary Lithium-Ion Battery Safety Standards, *Proceedings of the fourth IAASS Conference: Making Safety Matter*, Huntsville, AL, 2010.
11. J. Lamb and C. J. Orendorff, "Evaluation of mechanical abuse techniques in lithium ion batteries," *J. Power Sources*, **247**, 189 (2014).
12. W. Cai, H. Wang, H. Maleki, J. Howard, and E. Lara-Curzio, "Experimental simulation of internal short circuit in Li-ion and Li-ion-polymer cells," *J. Power Sources*, **196**, 7779 (2011).
13. IEEE 1625 IEEE Standard for Rechargeable Batteries for Multi-cell Mobile Computing Devices, 2008.
14. M. Keyser, D. Long, Y. S. Jung, and A. Pesaran, *Development of a Novel Test Method for On-Demand Internal Short Circuit in a Li-Ion Cell, Advanced Automotive Battery Conference*, Pasadena, CA, 2011.
15. G. Kim, M. Keyser, and A. Pesaran, DOE Vehicle Technologies Program Review, Project ID: ES109, 2011.
16. P. Ramadass, W. Fang, and Z. Zhang, "Study of internal short in a Li-ion cell I. Test method development using infra-red imaging technique," *J. Power Sources*, **248**, 769 (2014).
17. W. Fang, P. Ramadass, and Z. Zhang, "Study of internal short in a Li-ion cell-II. Numerical investigation using a 3D electrochemical-thermal model," *J. Power Sources*, **248**, 1090 (2014).
18. C. J. Orendorff, P. Roth, C. Carmignani, J. Langendorf, and L. Davis, *External Triggers for Internal Short Circuits in Lithium Ion Batteries, 215th ECS Meeting*, San Francisco, CA, 2009.
19. C. J. Orendorff, P. Roth, and T. Lambert, *Lithium-Ion Cell Safety Issues of Separators and Internal Short Circuits, 218th ECS Meeting*, Las Vegas, NV, 2010.
20. C. J. Orendorff, E. P. Roth, and G. Nagasubramanian, "Experimental triggers for internal short circuits in lithium-ion cells," *J. Power Sources*, **196**, 6554 (2011).
21. C. McCoy, M. Menard, M. C. Laupheimer, D. Ofer, B. Barnett, and S. Sriramulu, *Implantation, Activation, Characterization and Prevention/Mitigation of Internal Short Circuits in Lithium-Ion Cells*, DOE Annual Merit Review Meeting, 2012.
22. T. D. Hatchard, D. D. MacNeil, A. Basu, and J. R. Dahn, "Thermal Model of Cylindrical and Prismatic Lithium-ion Cells," *J. Electrochemical Society*, **147**, 755 (2001).
23. R. Spotnitz and J. Franklin, "Abuse Behavior of High-Power, Lithium-ion Cells," *J. Power Sources*, **113**, 81 (2003).
24. T. M. Bandhauer, S. Garimella, and T. F. Fuller, "A Critical Review of Thermal Issues in Lithium-ion Batteries," *J. Electrochemical Society*, **158**, 1 (2011).
25. P. Biensan, B. Simon, J. P. Peres, A. D. Guibert, M. Broussely, J. M. Bodet, and F. Perton, "On Safety of Lithium-ion Cells," *J. Power Sources*, **81–82**, 906 (1999).
26. T. G. Zavalis, M. Behm, and G. Lindbergh, "Investigation of Short-Circuit Scenarios in a Lithium-Ion Battery Cell," *J. Electrochem. Soc.*, **159**(6), A848 (2012).
27. L. Liu, X. He, L. Lu, M. Ouyang, M. Zhang, and X. Feng, *Evaluation of Triggering Approaches of Internal Short Circuit in Lithium Ion Batteries, 231st ECS Meeting*, New Orleans, LA, 2017.
28. J. Asakura, T. Nakashima, T. Nakatsuji, and M. Fujikawa, *Battery Internal Short-Circuit Detection Apparatus and Method, and Battery Pack*, US8334699.
29. K. Otsuka and C. M. Wayman, *Shape Memory Materials*, Cambridge Univ. Press, Cambridge, U.K., Nov. 1999.
30. A. Kriston, V. Ruiz, T. Kosmidou, J. Ungeheuer, H. Doring, B. Fritsch, A. Pfrang, and L. Boo-Brett, *Evaluation of External Short Circuit Performance of NCA and NCM Li-ion Batteries, 7th Annual Battery Safety*, Bethesda, MD, 2016.
31. M. Doyle, J. Newman, A. S. Gozdz, C. N. Schmulz, and J. M. Tarascon, "Comparison of Modeling Predictions with Experimental Data from Plastic Lithium Ion Cells," *J. Electrochem. Soc.*, **143**(6), 1890 (1996).
32. W. Zhao, G. Luo, and C. Wang, "Modeling Nail Penetration Process in Large-Format Li-ion Cells," *J. Electrochemical Society*, **162**, 207 (2015).
33. R. Spotnitz and J. Franklin, "Abuse Behavior of High-Power Lithium-ion cells," *J. Power Sources*, **113**, 81 (2003).
34. Engineering Toolbox, www.engineeringtoobox.com, Mar. 30th, 2017.
35. S. S. Zhang, "A review on the Separators of Liquid Electrolyte Li-ion Batteries," *J. Power Sources*, **164**, 351 (2007).